PCCP

Accepted Manuscript

ROYAL SOCIETY OF CHEMISTRY

www.rsc.org/pccp

Journal Name RSCPublishing

ARTICLE

Cite this: DOI: 10.1039/x0xx00000x

N Lone-pair···π Interaction: A Rotational Study of Chlorotrifluoroethylene···Ammonia

Qian Gou,[a] Lorenzo Spada,[a] Yannick Geboes,[b] Wouter A. Herrebout,[b] Sonia Melandri[a] and Walther Caminati[*,a]

Received 00th January 2012,
Accepted 00th January 2012

DOI: 10.1039/x0xx00000x

www.rsc.org/

The rotational spectra of four isotopologues of the adduct C_2F_3Cl-NH_3 show that NH_3 is bound to the partner molecule through a (N)lone pair···π interaction. Ammonia is located in proximity of the C2 atom (the one linked to two fluorine atoms), with the C2···N distance = 2.987(2) Å. The nuclear hyperfine structure due to the quadrupole coupling effects of $^{35}Cl/^{37}Cl$ and ^{14}N nuclei has been fully resolved. The ^{14}N quadrupole coupling constants allow estimating the effective orientation of NH_3 in the complex.

Introduction

The study of clusters involving simple molecules, such as water or ammonia, has attracted considerable attention as a model for investigating the nature of the non covalent interactions which link these simple (solvent) species to the partner molecules.

A considerable number of complexes with water have been investigated. It has been found that water either acts as a proton-acceptor or as a proton-donor or even has a dual role, thereby forming several types of hydrogen bonds (HBs). A classification of the kind of HBs and of the internal dynamics of water in its molecular complexes is given in a recent paper.[1] With aliphatic perhalogenated molecules (in which no hydrogen atoms are present), however, a halogen bond (HaB), rather than a HB is formed.[2, 3] Details of the nature of the HaB in the gas phase can be obtained by rotational spectroscopy of molecular complexes, as shown in some review or perspective articles by Legon.[4] More recently, we have shown, through the rotational spectrum of chlorotrifluoroethylene (C_2F_3Cl, freon-1113) –water, that water links to a fully halogenated alkene through a lone-pair (*lp*)···π interaction.[5]

Less information is available on molecular complexes of ammonia with organic molecules. Ammonia, similarly to water, possesses slightly acidic protons and a lone pair. It has been indicated that NH_3 can act as a proton acceptor[6] or as a donor[7] or even assume a dual role[8] to form HBs with organic molecules. When forming a complex with a perhalogenated saturated freon like CF_3Cl, NH_3 acts as a halogen acceptor to form a Cl···N HaB[9] resulting from the "σ-hole",[10] and has an internal dynamic behaviour similar to that of water in $CF_3Cl\cdots H_2O$.[3]

No adducts of NH_3 with perhalogenated unsaturated freons have been investigated by rotational spectroscopy. In such kind of freons, a positive electrostatic potential region is formed above the molecular framework (π-hole)[10] due to the electron withdrawing by the covalently bonded halogen atoms. As mentioned above, in C_2F_3Cl-H_2O an oxygen *lp*···π interaction represents the leading attraction.[5] Will NH_3 behave in the same way (forming a N *lp*···π interaction) in C_2F_3Cl-NH_3? A similar effect, the Bürgi-Dunitz *n*-π* interaction has been found to stabilize one or two conformers in amino acids. In the case of *β*-alanine, one conformer of the four observed ones (the highest in energy) is stabilized by such a linkage rather than an intramolecular HB.[11] In the case of γ-aminobutyric acid, two conformers (including the most stable one) of the nine conformers present this intramolecular interaction.[12] Finally, the *n*-π* interaction is considered responsible for the thermal conversion of 5-aminovaleric acid to δ-valerolactam.[13] *lp*–π interactions have been reported to be among the factors stabilizing supramolecular assemblies.[14]

In this paper, we report the rotational study of the complex C_2F_3Cl-NH_3 with the Fourier transform microwave technique. Furthermore, a precise determination of the effective orientation of NH_3 has been made using the ^{14}N quadrupolar coupling constants.

Experimental Section

Molecular clusters were generated in a supersonic expansion, under conditions optimized for the dimer formation. Details of the Fourier transform microwave spectrometer[15] (COBRA-type[16]), which covers the range 6.5-18 GHz, have been described previously.[17]

A gas mixture of ca. 1% of C_2F_3Cl and NH_3 or $^{15}NH_3$ (10%) or ND_3 (99%) purchased from Aldrich, in helium at a stagnation pressure of ~ 0.5 MPa was expanded through a solenoid valve (General Valve, Series 9, nozzle diameter 0.5 mm) into the Fabry-Pérot cavity. The spectral line positions were determined after Fourier transformation of the time-domain signal with 8k data points, recorded with 100 ns sample intervals. Each rotational transition appears as a doublet due to Doppler Effect. The line position is calculated as the arithmetic mean of the frequencies of the Doppler components. The estimated accuracy of the frequency measurements is better than 3 kHz. Lines separated by more than 7 kHz are resolvable.

Theoretical calculations

Before collecting the rotational spectra, full geometry optimizations of the complex were carried out with *ab initio* calculation at the MP2/aug-cc-pVDZ level using the Gaussian09 program package.[18] Two plausible isomers were found to be real minima by the vibrational frequency calculations which also give the zero-point corrected energies (ZPE). In order to have a better estimate of the energy differences, both intermolecular binding energy values were counterpoise corrected for basis set superposition error (BSSE).[19] In addition, the ZPE dissociation energies have been estimated, including BSSE corrections. The corresponding geometries, as well as the calculated rotational and quadrupole coupling constants, electric dipole moment components and relative energies are listed in Table 1. From this data it is clear that the *lp*···π bonded isomer **I** is more stable than the Cl···N HaB bonded isomer **II**.

Table 1 MP2/aug-cc-pVDZ calculated parameters of the two plausible isomers of C_2F_3Cl-NH_3.

	I	II
$\Delta E,\Delta E_{ZPE},\Delta E_{BSSE}/cm^{-1}$	0,0,0[a]	330,331,44
A,B,C/MHz	2191,1281,1192	3839,862,706
$\chi_{aa}(Cl),\chi_{bb}-\chi_{cc}(Cl)$/MHz	-20.9,-45.2	-65.9,-2.7
$\chi_{ab}(Cl),\chi_{bc}(Cl),\chi_{ac}(Cl)$/MHz	-50.3,6.3,5.7	-18.1,0.0,0.0
$\chi_{aa}(N),\chi_{bb}-\chi_{cc}(N)$/MHz	-0.3,0.3	-3.3,-0.2
$\chi_{ab}(N),\chi_{bc}(N),\chi_{ac}(N)$/MHz	1.8,1.9,-1.6	-0.9,0.0,0.0
$\|\mu_a\|,\|\mu_b\|,\|\mu_c\|$/D	1.1,1.4,0.8	2.7,0.6,0.0
E_D/kJ mol^{-1}	7.5	7.0
	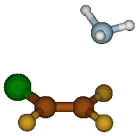	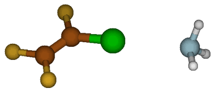

[a] Absolute energies are -890.979805, -890.926933 and -890.982202 E_h, respectively.

The rotational spectrum was expected to be quite complicated due to the two quadrupolar nuclei $^{35}Cl/^{37}Cl$ ($I = 3/2$) and ^{14}N ($I = 1$) leading each transition to split into many (typically 12 relatively intense) component lines. Additionally, the almost free internal rotation of NH_3, with a calculated barrier of only ~2 cm^{-1} might generate observable torsional satellites.

Rotational spectra

Following the predictions from the theoretical calculations, we searched first for the μ_a-type R band transitions of isomer **I**. Transitions with J_{upper} = 3 to 7 and with K_{-1} up to 3 have been assigned to isomer **I** according to the corresponding quadrupolar pattern, as shown, for example, in Fig. 1 for the $3_{13}\leftarrow 2_{12}$ transition. Then some stronger μ_b-type R and weaker μ_c-type R branch lines were also identified.

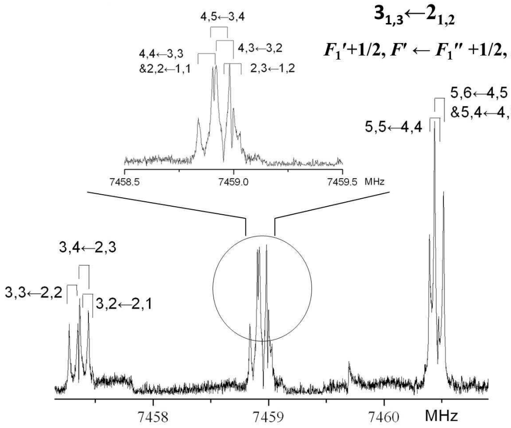

Fig. 1 ^{35}Cl and ^{14}N quadrupole hyperfine structure of the $3_{13}\leftarrow 2_{12}$ transition of $C_2F_3{}^{35}Cl$-$^{14}NH_3$. Each line appears as a doublet (⊓) due to the Doppler effect.

Finally, it was possible to fit 475 measured lines using Pickett's SPFIT program,[20] according to the following Hamiltonian:

$$H = H_R + H_{CD} + H_Q \qquad (1)$$

where H_R represents the rigid rotational parts of the Hamiltonian, the centrifugal distortion contributions (analyzed using the S reduction and I^r representation)[21] are represented by H_{CD} and H_Q is the operator associated with the $^{35}Cl/^{37}Cl$ and ^{14}N quadrupolar interaction. The obtained spectroscopic parameters are summarized in the first column of Table 2.

A weaker set of transitions was observed at lower frequencies, and after the empirical adjustment to the molecular structure, it was possible to assign them to the $C_2F_3{}^{37}Cl$-$^{14}NH_3$ isotopologue. The intensities of these transitions were about 1/3 of those of the parent species, which is consistent with the natural relative abundance of the two isotopes. Due to the lower intensities, fewer lines have been measured for the $C_2F_3{}^{37}Cl$-$^{14}NH_3$ isotopologue; as a consequence, the ^{14}N quadrupolar coupling constants and some centrifugal distortion constants could not be well determined and have been fixed at the corresponding values of the parent species. The obtained experimental parameters are summarized in the right column of Table 2.

Table 2 Experimental spectroscopic parameters of $C_2F_3{}^{35}Cl$-$^{14}NH_3$ and $C_2F_3{}^{37}Cl$-$^{14}NH_3$ (S-reduction, I^r representation)

	$C_2F_3{}^{35}Cl$-$^{14}NH_3$	$C_2F_3{}^{37}Cl$-$^{14}NH_3$
A/MHz	2236.0689(1)[a]	2225.110(1)
B/MHz	1317.19498(8)	1294.36090(8)
C/MHz	1219.63324(7)	1196.9012(1)
$\chi_{aa}(Cl)$/MHz	-21.817(2)	-18.71(1)
$\chi_{bb}-\chi_{cc}(Cl)$/MHz	-50.762(4)	-38.630(7)
$\chi_{ab}(Cl)$/MHz	55.9(4)	46.1(8)
$\chi_{bc}(Cl)$/MHz	12(2)	-
$\chi_{ac}(Cl)$/MHz	10.3(3)	6.8(5)
$\chi_{aa}(N)$/MHz	-0.404(2)	[-0.404][b]
$\chi_{bb}-\chi_{cc}(N)$/MHz	-0.435(4)	[-0.435]
$\chi_{ab}(N)$/MHz	0.72(6)	[0.7]
$\chi_{ac}(N)$/MHz	1.8(4)	[1.8]
D_J/kHz	2.5186(8)	2.416(1)
D_{JK}/kHz	-6.710(6)	-6.27(7)

D_K/kHz	16.926(9)	[16.926]
d_1/kHz	-0.3695(8)	[-0.3695]
d_2/kHz	-0.1151(9)	[-0.1151]
σ^c/kHz	2.8	3.5
N^d	475	176

[a] Error in parentheses in units of the last digit; [b] Numbers in brackets are fixed to the corresponding value of the parent species. [c] Standard deviation of the fit; [d] Number of lines in the fit.

Furthermore, using samples of $^{15}NH_3$ (10%) and $^{14}ND_3$ (99%), the rotational spectra of two further isotopologues have been measured and assigned. Their experimental spectroscopic parameters have been listed in Table 3. The intensities of the transitions of the isotopologue $C_2F_3{}^{35}Cl$-$^{15}NH_3$ are about 3/10 of the corresponding transitions of the parent species, since ^{15}N (I = 1/2) will not generate any quadrupolar splitting. For the isotopologue $C_2F_3{}^{35}Cl$-$^{14}ND_3$, the presence of three deuterium nuclei (I = 1) with very small nuclear electric quadrupole moments (Q), leads to further splitting of rotational transitions. However, such a hyperfine structure is not resolved with our spectrometer, resulting in a broadening of the lines and a decrease of their intensities. The quadrupolar coupling constants of $C_2F_3{}^{35}Cl$-$^{14}ND_3$ are quite different from those of the parent species, due to a reorientation of the principal axis system upon the triple isotopic substitution.

Table 3 Experimental spectroscopic parameters of $C_2F_3{}^{35}Cl$-$^{15}NH_3$ and $C_2F_3{}^{35}Cl$-$^{14}ND_3$ (S-reduction, I^r representation)

	$C_2F_3{}^{35}Cl$-$^{15}NH_3$	$C_2F_3{}^{35}Cl$-$^{14}ND_3$
A/MHz	2205.243(3)^a	2129.536(3)
B/MHz	1295.0543(6)	1234.8271(5)
C/MHz	1198.5099(4)	1138.5060(3)
χ_{aa}(Cl)/MHz	-19.85(4)	-14.33(1)
χ_{bb}-χ_{cc}(Cl)/MHz	-51.78(3)	-51.82(1)
χ_{ab}(Cl)/MHz	[55.9]^b	56.9(9)
χ_{bc}(Cl)/MHz	[12]	[12]
χ_{ac}(Cl)/MHz	[10.3]	17.8(4)
χ_{aa}(N)/MHz	-	-0.936(7)
χ_{bb}-χ_{cc}(N)/MHz	-	-1.09(1)
χ_{ab}(N)/MHz	-	3.2(5)
χ_{ac}(N)/MHz	-	[1.8]
D_J/kHz	2.547(5)	2.654(4)
D_{JK}/kHz	-7.4(1)	-9.2(1)
D_K/kHz	[16.926]	[16.926]
d_1/kHz	-0.414(5)	-0.589(4)
d_2/kHz	[-0.1151]	[-0.1151]
σ^c/kHz	2.7	3.1
N^d	51	120

[a] Error in parentheses in units of the last digit; [b] Fixed at the value of the parent species. [c] Standard deviation of the fit; [d] Number of lines in the fit.

All measured transition frequencies are available in ESI.†

Conformational assignment

The experimental spectroscopic parameters in Table 2 match the theoretical values of form **I** in Table 1, which is stabilized by the N $lp\cdots\pi$ interaction. An additional search was performed in an attempt to observe lines belonging to isomer **II**. However, despite the small difference in the conformational energy, no such lines were observed. This could be due to the conformational relaxation to the most stable isomer upon supersonic expansion. It has, indeed, been shown that this kind of relaxation takes place easily when the interconversion barrier is smaller than $2kT$,[22] where T is the temperature before supersonic expansion; $2kT$ is about 410 cm^{-1} at 25°C, which is the pre-expansion temperature in our case. We measured only transitions belonging to the $m = 0$ torsional state.

Further efforts to find $m \neq 0$ lines have been made but were unsuccessful, probably due to the huge splitting resulting from the rather low barrier (see the discussion ahead) of rotation of NH_3.

Molecular structure

The configuration of the observed isomer is shown in Fig. 2, including the principal axes and atom numbering. X8 is a dummy atom in the symmetric axis of NH_3 to indicate its orientation. NH_3, similar to H_2O, prefers to locate above the C2 atom (the one attached to two F atoms) of C_2F_3Cl, due to the stronger electron withdrawing effect of fluorine as compared to chlorine, forming a N $lp\cdots\pi$ interaction.

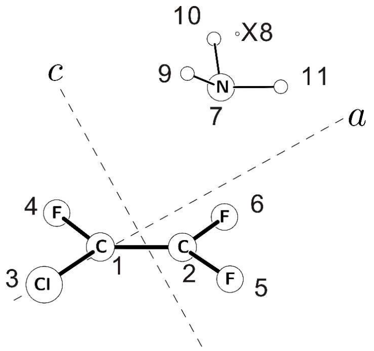

Fig. 2 The observed isomer with principal axes and the atom numbering. X8 is a dummy atom in the symmetric axis of NH_3.

From the rotational constants of the three isotopologues $C_2F_3{}^{35}Cl$-$^{14}NH_3$, $C_2F_3{}^{37}Cl$-$^{14}NH_3$ and $C_2F_3{}^{35}Cl$-$^{15}NH_3$, it is possible to calculate the r_s substitution coordinates[23] of the Cl and N atoms in the principal axes of the parent species. The obtained values are shown in Table 4, and are compared with the values of a partial r_0 structure.

Table 4 The experimental coordinates of the Cl and N atoms in C_2F_3Cl-NH_3

		a/Å	b/Å	c/Å
Cl	r_s	±1.847(1)	±0.766(2)	±0.06(3)
	$r_0{}^a$	-1.881	0.724	0.027
N	r_s	±2.304(1)	±1.400(1)	±1.155(1)
	$r_0{}^a$	2.156	1.269	-1.385

[a] Calculated with the partial r_0 structure in Table 5.

The partial r_0 structure was obtained by adjusting three structural parameters (R_{N7C2}, ∠N7···C2C1 and ∠N7···C2C1Cl3), while keeping the remaining parameters fixed to their *ab initio* values in order to reproduce the experimental rotational constants. The obtained parameters, as well as the corresponding *ab initio* values, are reported in Table 5.

Table 5 Partial r_0 and r_e structures of C_2F_3Cl-NH_3

	R_{N7C2}/Å	∠N7C2C1/°	∠N7C2C1Cl3/°
r_0	2.987(2)[a]	100.9(1)	88.3(1)
r_e	3.103	101.5	89.0

[a] Uncertainties (in parentheses) are expressed in units of the last digit.

Internal dynamics

This "mixed" structure (given as ESI†) effectively provides good agreement with the experimental values but not for $C_2F_3{}^{35}Cl$-${}^{14}ND_3$. The discrepancy of rotational constant A of $C_2F_3{}^{35}Cl$-${}^{14}ND_3$ is as large as 30 MHz. This effect is often associated to an almost free internal rotation of a heavy top,[24] and it can be explained by taking into account the influence of the internal rotation on the values of the effective rotational constants of the ground state ($v = 0$, $\sigma = 0$), according to:[25]

$$\begin{aligned} A_{00} &= A_r + W_{00}^{(2)} F\rho_a^2 \\ B_{00} &= B_r + W_{00}^{(2)} F\rho_b^2 \\ C_{00} &= C_r + W_{00}^{(2)} F\rho_c^2 \end{aligned} \qquad (2)$$

where A_r, B_r and C_r are the "rigid" rotational constants in the limit of both infinite barriers. The $W_{00}^{(2)}$ are the Herschbach's barrier-dependent perturbation sums relative to the sublevels of the A-symmetry ($\sigma = 0$) species of the torsional ground state ($v = 0$) with $\rho_g = \lambda_g I_\alpha / I_g$ depending on the moments of inertia along the symmetry axis α of the internal rotor and the principal axis g and their directional cosine λ_g, while $F = \hbar/[2\cdot(1-\Sigma_g \lambda_g I_\alpha/I_g)I_\alpha]$ is the reduced constant of the motion. Tables of the $W_{00}^{(n)}$ as a function of the reduced barrier s are available.[25] The parameter s is, in turn, related to the V_3 barrier according to: $V_3 = 0.215\cdot s\,F$. Applying the differences between the parent and tri-deuterated species, $W_{00}^{(2)}$ has been estimated to be ~2.6 according to:

$$\Delta A_{00} = \Delta A_r + W_{00}^{(2)} \Delta F\rho_a^2 \qquad (3)$$

Such large value of $W_{00}^{(2)}$ corresponds to $s \approx 0$ therefore indicating that NH_3 undergoes an almost free internal rotation.

Effective orientation of NH_3

Determination of the effective orientation of NH_3 (the effective values of ∠X8N7C2 and ∠X8N7C2C1) is not possible using the usual structure fitting. The partial r_0 geometry given above does, indeed, not provide the experimental ${}^{14}N$ quadrupole coupling constants. As mentioned in the previous studies, similar effects have been sized in several complexes of NH_3, based on the experimental values of the quadrupole coupling constants of ${}^{14}N$.[8,9] By adjusting the two orientation angles, we succeeded in reproducing the experimental values of $\chi_{aa}({}^{14}N)$ and χ_{bb}-$\chi_{cc}({}^{14}N)$ with MP2/aug-cc-pVDZ level calculations. The results are shown in Table 6, where the adjusted and r_0 values of the two angles and the corresponding ${}^{14}N$ quadrupole coupling constants are also given. In ESI,† the changes of the quadrupole coupling constants as functions of the two angles are summarized in two tables.

Table 6 Effective orientation of NH_3 in C_2F_3Cl-NH_3 which reproduces the experimental values of the ${}^{14}N$ quadrupole coupling constants.

	∠X8N7C2/°	∠X8N7C2C1/°	χ_{aa}(N)/MHz	χ_{bb}-χ_{cc}(N)/MHz
Adjusted	166.1(1)[a]	138.6(1)	-0.404	-0.436
r_0	176.2	154.8	-0.174[b]	1.001

[a] Uncertainties (in parentheses) are expressed in units of the last digit; [b] Calculated with the partial r_0 structure in Table 5 at MP2/aug-cc-pVDZ

Conclusions

This rotational study of C_2F_3Cl-NH_3 and of its isotopologues points out irrefutably that the (N)*lp* of NH_3, similarly to the (O)*lp* in water is linked to the π system of the partner molecule C_2F_3Cl. The nuclear quadrupole hyperfine structure due to ${}^{14}N$ and ${}^{35}Cl/{}^{37}Cl$ nuclei considerably complicates the rotational spectrum but its analysis provides useful information on the structure and internal dynamics of the complex. In addition, the values of the ${}^{14}N$ quadrupole coupling constants allow for the estimation of the effective orientation of NH_3 in the complex.

This study provides further interesting experimental evidence on the nature of *lp*···π interaction obtained by rotational spectroscopy.

Ammonia is linked to the π-system, but in the proximity of the C2 carbon atom, with a C2···N distance of 2.987(2) Å. The preferred location of ammonia is probably due to the π-hole around the C2 carbon, generated by the higher electro negativity of F with respect to Cl.

In addition, from the value of the rotational constant A of $C_2F_3{}^{35}Cl$-${}^{14}ND_3$, higher than expected just from the replacement of NH_3 with ND_3 with respect to that of $C_2F_3{}^{35}Cl$-${}^{14}NH_3$, we could deduce that the V_3 barrier to internal rotation of NH_3 around its symmetry axis is close to zero.

Acknowledgements

Financial support has been provided by: Italian MIUR (PRIN project 2010ERFKXL_001), University of Bologna (RFO), FWO-Vlaanderen, the Special Research Fund BOF and the Hercules foundation. Q. G. thanks the China Scholarships Council (CSC) for financial support. Y.G. would also like to thank FWO-Vlaanderen for awarding him a research fellowship (11O9514N).

Notes and references

[a] Dipartimento di Chimica "G. Ciamician" dell'Università, Via Selmi 2, I-40126 Bologna, Italy.

[b] Department of Chemistry, University of Antwerp, Groenenborgerlaan 171, 2020 Antwerp, Belgium.

.

†Electronic Supplementary Information (ESI) available: [details of any supplementary information available should be included here]. See DOI: 10.1039/b000000x/

1 L. Evangelisti and W. Caminati, *Phys. Chem. Chem. Phys.*, 2010, **12**, 14433.

2 W. Caminati, A. Maris, A. Dell'Erba and P. G. Favero, *Angew. Chem. Int. Ed.*, 2006, **45**, 6711.

3 L. Evangelisti, G. Feng, P. Écija, E. J. Cocinero, F. Castaño and W. Caminati, *Angew. Chem. Int. Ed.*, 2011, **50**, 7807.

4 A. C. Legon, *Phys. Chem. Chem. Phys.*, 2010, **12**, 7736.

5 Q. Gou, G. Feng, L. Evangelisti and W. Caminati, *Angew .Chem. Int. Ed.*, 2013, **52**, 11888.

6 G. T. Fraser, F. J. Lovas, R. D. Suenram, D. D., Jr. Nelson and W. Klemperer, *J. Chem. Phys.*, 1986, **84**, 5983; G. T. Fraser, R. D.

Suenram, F. J. Lovas and W. Stevens, *J. Chem. Phys.*, 1988, **125**, 31; C. Rensing, H. Mäder and F. Temps, *J. Mol. Spectrosc.*, 2008, **251**, 224; B. M. Giuliano, M. C. Castrovilli, A. Maris, S. Melandri, W. Caminati and E. A. Cohen, *Chem. Phys. Lett.*, 2008, **463**, 330.

7 D. A. Rodham, S. Suzuki, R. D. Suenram, F. J. Lovas, S. Dasgupta, W. A. Goddard III and G. A. Blake, *Nature*, 1993, **362**, 735.

8 C. Tanner, C. Manca and S. Leutwyler, *Science*, 2003, **302**, 1736; B. M. Giuliano, S. Melandri, A. Maris, L. B. Favero and W. Caminati, *Angew. Chem. Int. Ed.*, 2009, **48**, 1102; B. M. Giuliano, A. Maris, S. Melandri and W. Caminati, *J. Phys. Chem. A*, 2009, **113**, 14277; J. Thomas, O. Sukhorukov, W. Jäger and Y. Xu, *Angew. Chem. Int. Ed.,* 2013, **52**, 4402; B. M. Giuliano, L. Evangelisti, A. Maris and W. Caminati, *Chem. Phys. Lett.*, 2010, **485**, 36; S. Melandri, A. Maris and L. B. Favero, *Mol. Phys*., 2010, **108**, 2219.

9 G. Feng, L. Evangelisti, N. Gasparini and W. Caminati, *Chem. Eur. J.*, 2012, **18**, 1364.

10 See for example, J. S. Murray, P. Lane, T. Clark, K. E. Riley, P. Politzer, *J. Mol. Model.*, 2012, **18**, 541.

11 M. E. Sanz, A. Lesarri, M. I. Peña, V. Vaquero, V. Cortijo, J. C. López and J. L. Alonso, *J. Am. Chem. Soc*., 2006, **128**, 3812.

12 S. Blanco, J. C. López, S. Mata and J. L. Alonso, *Angew. Chem. Int. Ed*., 2010, **49**, 9187.

13 R. G. Bird, V. Vaquero-Vara, D. P. Zaleski, B. H. Pate, D. W. Pratt, *J. Mol. Spectrosc.*, 2012, **280**, 42.

14 A. Das, S. R. Choudhury, B. Dey, S. K. Yalamanchili, M. Helliwell, P. Gamez, S. Mukhopadhyay, C. Estarellas, A. Frontera, *J. Phys. Chem. B*, 2010**, 114***,* 4998; A. Das, S. R. Choudhury, C. Estarellas, B. Dey, A. Frontera, J. Hemming, M. Helliwell, P. Gamez, S. Mukhopadhyay, *CrystEngComm*, 2011, **13**, 4519; P. Manna, S. K. Seth, A. Das, J. Hemming, R. Prendergast, M. Helliwell, S. R. Choudhury, A. Frontera, S. Mukhopadhyay, *Inorg. Chem*., 2012, **51**, 3557.

15 T. J. Balle, W. H. Flygare, *Rev. Sci. Instrum.*, 1981, **52**, 33.

16 J.-U. Grabow, W. Stahl and H. Dreizler, *Rev. Sci. Instrum.*, 1996, **67**, 4072.

17 W. Caminati, A. Millemaggi, J. L. Alonso, A. Lesarri, J. C. Lopez and S. Mata, *Chem. Phys. Lett.*, 2004, **392**, 1.

18 M. J. Frisch, G. W. Trucks, H. B. Schlegel, G. E. Scuseria, M. A. Robb, J. R. Cheeseman, G. Scalmani, V. Barone, B. Mennucci, G. A. Petersson, H. Nakatsuji, M. Caricato, X. Li, H. P. Hratchian, A. F. Izmaylov, J. Bloino, G. Zheng, J. L. Sonnenberg, M. Hada, M. Ehara, K. Toyota, R. Fukuda, J. Hasegawa, M. Ishida, T. Nakajima, Y. Honda, O. Kitao, H. Nakai, T. Vreven, J. A. Montgomery, Jr., J. E. Peralta, F. Ogliaro, M. Bearpark, J. J. Heyd, E. Brothers, K. N. Kudin, V. N. Staroverov, R. Kobayashi, J. Normand, K. Raghavachari, A. Rendell, J. C. Burant, S. S. Iyengar, J. Tomasi, M. Cossi, N. Rega, J. M. Millam, M. Klene, J. E. Knox, J. B. Cross, V. Bakken, C. Adamo, J. Jaramillo, R. Gomperts, R. E. Stratmann, O. Yazyev, A. J. Austin, R. Cammi, C. Pomelli, J. W. Ochterski, R. L. Martin, K. Morokuma, V. G. Zakrzewski, G. A. Voth, P. Salvador, J. J. Dannenberg, S. Dapprich, A. D. Daniels, Ö. Farkas, J. B. Foresman, J. V. Ortiz, J. Cioslowski, and D. J. Fox, Gaussian, Inc., Wallingford CT, **2009**.

19 S. F. Boys, F. Bernardi, *Mol. Phys.*, 1970, **19**, 553.

20 M. H. Pickett, *J. Mol. Spectrosc.*, 1991, **148**, 371.

21 J. K. G. Watson, in Vibrational Spectra and structure, Vol. 6 (Ed: J. R. Durig), ELSEVIER, New York/Amsterdam, 1977, pp.1-89.

22 See for example: R. S. Ruoff, T. D. Klots, T. Emilson, H. S. Gutowski, *J. Chem. Phys.*, 1990, **93**, 3142.

23 J. Kraichman, *Am. J. Phys.*, 1953, **21**, 17.

24 See, for example, Q. Gou, L. Spada, E. J. Cocinero and W. Caminati, *J. Phys. Chem. Lett.*, 2014, **5**, 1591.

25 D. R. Herschbach, *J. Chem. Phys.*, 1959, **31**, 91.